

14 Mar 1991, 10:30 am - 12:30 pm

Influence of Liquefaction to Pile-Soil-Structure Interaction

Tadahiko Shiomi
Takenaka Corporation, Japan

Michlo Sugumoto
Takenaka Corporation, Japan

Yoshimasa Shigeno
Takenaka Corporation, Japan

Yoshio Suzuki
Takenaka Corporation, Japan

Follow this and additional works at: <https://scholarsmine.mst.edu/icrageesd>



Part of the [Geotechnical Engineering Commons](#)

Recommended Citation

Shiomi, Tadahiko; Sugumoto, Michlo; Shigeno, Yoshimasa; and Suzuki, Yoshio, "Influence of Liquefaction to Pile-Soil-Structure Interaction" (1991). *International Conferences on Recent Advances in Geotechnical Earthquake Engineering and Soil Dynamics*. 25.

<https://scholarsmine.mst.edu/icrageesd/02icrageesd/session03/25>

This Article - Conference proceedings is brought to you for free and open access by Scholars' Mine. It has been accepted for inclusion in International Conferences on Recent Advances in Geotechnical Earthquake Engineering and Soil Dynamics by an authorized administrator of Scholars' Mine. This work is protected by U. S. Copyright Law. Unauthorized use including reproduction for redistribution requires the permission of the copyright holder. For more information, please contact scholarsmine@mst.edu.

Influence of Liquefaction to Pile-Soil-Structure Interaction

Tadahiko Shiomi
Technical Research Laboratory, Takenaka Corporation

Yoshimasa Shigeno
Technical Research Laboratory, Takenaka Corporation

Michio Sugumoto
Technical Research Laboratory, Takenaka Corporation

Yoshio Suzuki
Technical Research Laboratory, Takenaka Corporation

SYNOPSIS: Influence of liquefaction on a pile-soil-structure interaction is studied by a dynamic effective analysis code (MuDIAN). The soil properties are modeled by a Mohr-Coulomb assumption with a dilatancy model. Liquefaction takes place in shallow depth and cause the change of dynamic behavior. The approaches, evaluation method of soil constants and results are reported in details.

INTRODUCTION

Countermeasures of the ground liquefaction is one of the most urgent problems for near-seaside developments in earthquake country such as Japan. To solve this problem, authors have long been studying the numerical approaches for the liquefaction phenomena, i.e. governing equations, finite formulations, constitutive equations for sands and surveyed the phenomena by analyzing problems of ground layers, dams, soil-structures, etc. The approaches have been verified with many experiments and observation. In this paper, we report effects of liquefaction on dynamic behavior of pile-soil-structure systems using our approaches.

Behaviour of piles subjected to lateral forces is complicate problem even without liquefaction phenomena. Effects of multi-layer of soils, grouping and rigidity of foundation are main research works. A simple way of analyses has been proposed by Penzien [1970], Gazetas and Dobry [1984], Kausel and Banerjee [1985], Ahn and Gould [1986] and many others. The most approaches use "beam-on-Winkler-foundation" model where nonlinearity of soil is considered by nonlinear springs. None of them considered weakening of soil material due to liquefaction. Finite Element Method and Boundary Element Method are also used to study those problems such as Desai and Kuppasamy [1980] and Kausel and Banerjee [1985].

Implementation of liquefaction effect into Penzien's method is attempted by Muto [1990]. One dimensional dynamic liquefaction analyses, DESRA [Finn et al 1977] and YUSAYUSA [Ishihara and Towhata 1980], are used separately to calculate pore pressure build-up and reduction of mean effective stress. But one dimensional analysis can not correctly interpret the pore pressure built-up since interaction behavior of soils and pile-structure are not taken into account.

The initial stresses act important role in the liquefaction. Therefore the initial stress was calculated taking into account generation of the static state such as settlements or sedimentation by self-weight for plane ground and thereafter the construction stage. And it was founded that overburden of the building plays important role for liquefaction of the soil under the building.

We report on a constitutive model from the engineering point of view. The model is easy to handle for practicing engineer because the constitutive model is function of a independent parameters such as shear failure and dilatancy behavior. Mohr-Coulomb criterion is used for the shear failure criterion. The parameters of the criterion are wellknown for engineers and are used in everyday practice. And endochronic type model is added for dilatancy and pore pressure build-up. This model is surveyed with many laboratory tests [Tanaka and Yasunaka 1982 and many others].

NUMERICAL METHOD

To survey influence of liquefaction to "pile-soil-structure" problem we adopted a dynamic effective stress analysis method based on two phase mixed theory (Zienkiewicz and Shiomi 1984). The two phase theory installed into a finite element code (MuDIAN) using u-U formulation in which two unknown variables are displacements for both solid (u) and fluid (U) phase. Isoparametric beam element and plain strain two dimensional element are adopted in order to model the frame structure of building, piles and ground.

Stage Analysis

Initial condition of stress are calculated before dynamic analysis is conducted by static "stage analysis". A procedure of building construction is shown in fig. 1.

- Step 1: Obtain a plain ground
- Step 2: Excavate for basement
- Step 3: Construct piles and then building

The construction process is followed by "stage analysis" in order to calculate the initial situation of a problem. The stage analysis is done by deleting soil elements of ground and adding beam elements of piles and frame buildings (Fig.1).

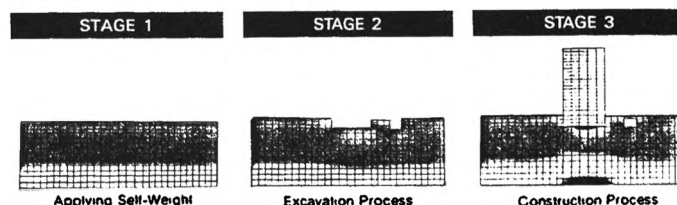


Figure 1: Example of Construction Process

Constitutive Model

To represent the dilatancy behavior which cause the liquefaction, we adopt "Densification Model" (Zienkiewicz et al 1978) for the stress-strain relationship modeling. This model is simple and easy to understand for ordinary engineers. Since engineers are often use "the Mohr-Coulomb or Tresca type" elasto- plastic relationship and the "Densification model" independently adds an additional function of dilatancy. Here we review the method.

The pore pressure built-up is often observed with cyclic loading and the relationship between pore pressure and number of cycles are

often investigated. Those relationship is generalized by Zienkiewicz (1978) and the following equations are introduced with autogeneous volumetric strain. The autogeneous strain is strain translated from pore pressure built-up during cyclic loading on undrained condition. To develop algorithm this following formulas are adopted.

$$d\sigma'_{ij} = D_{ijkl}^T (d\epsilon_{kl} - \frac{\delta_{kl} d\epsilon_v^o}{3}) \quad (1)$$

where $d\epsilon_v^o$ is the incremental autogeneous strain and D_{ijkl} is the drained elasto-plastic constitutive equation. When no change of total stress occurs

$$dp = -(\frac{1}{K_f} + \frac{n}{K_f})^{-1} d\epsilon_v^o \quad (2)$$

where K_f is the fluid bulk modulus, K_T is the bulk tangential and n is porosity. The cumulative autogeneous volumetric strain can be expressed as a function of the stress ratio θ and the length of the total straining path ξ . The incremental form of ξ is defined as

$$d\xi = (\frac{1}{2} d\epsilon_{ij} d\epsilon_{ij})^{\frac{1}{2}} \quad (3)$$

where $d\epsilon_{ij}$ is the incremental deviatoric strain. The autogeneous strain can be measured as a kind of endochronic strain (Bazant 1976), but here no time effect and total strain are adopted rather than separation of plastic strain. The incremental autogeneous strain can be written as

$$d\epsilon_v^o = -\frac{A}{1+B\kappa} d\kappa \quad (4)$$

where

$$d\kappa = e^{\gamma\theta} d\xi \quad (5)$$

The stress ratio θ defined as $\theta = \frac{\sigma'}{\sigma'_{mo}}$ where σ' is the second effective stress invariant and σ'_{mo} is the average effective mean stress at the start of cycling, i.e., $\sigma' = (\frac{1}{2} S_{ij} S_{ij})^{\frac{1}{2}}$ and $S_{ij} = \sigma_{ij} - \delta_{ij} \sigma_{kk}/3$

The those relation the procedure will be as follows.

- evaluate total strain $d\epsilon$
- evaluate total strain path $d\xi$ by Eq. (3)
- evaluate the damage parameter $d\kappa$ by Eq. (5)
- evaluate the autogeneous strain $d\epsilon_v^o$ by Eq. (4)
- evaluate the effective stress $d\sigma'$ by Eq. (1)
- evaluate the pore pressure dp in fluid phase.

One drawback of this method is that global tangential stiffness can not explicitly be obtained since Eqs.(3), (4) and (5) are not linear. So explicit time integration scheme or initial stiffness method of implicit time integration scheme should be adopted in which the tangential stiffness is not need. Here we adopt the implicit scheme.

PILE-SOIL-STRUCTURE INVESTIGATED

A pile-soil-structure system is surveyed for liquefaction phenomena. A structural part is a tall building near Sumida river in Tokyo. The problem is taken from a real construction project. The building is 19 story apartment near Sumida river where the ground is soft and liquefaction is anticipated. But the problem is slightly modified to produce full liquefaction by changing material properties of soil. Fig. 2 shows the overview of the problem. The building is 32m x 32m in plan and supported by 6 x 6 reinforced concrete piles. Bed rock is located at 40m depth and 16.5m thick sandy layer are located at -3.5m to -20m where liquefaction probably take place. The problems is modeled as a two dimensional problem so 6.4m span is modeled taking one column story.

The finite element model can be seen in Fig. 5 which shows vibration modes. In the model, right and left side boundaries are tied

each other, i.e. the pile-soil-structure model is same as a model that a mirror image configuration appears repeatedly at the both sides. The model has a adjacent building with distance of 120m for both sides. The building is a steel frame structure. Its foundation is made of reinforced concrete. Tables 1 and 2 show the structural properties i.e. column and beam respectively.

Table 1: Material Properties of Building (Column)

Floor	A (m ²)	I (m ⁴)	ν	E (tonf/m ²)
16 - 19F	0.0473	1.46x10 ⁻³	0.3	2.1x10 ⁷
8 - 15F	0.0544	2.02x10 ⁻³	0.3	2.1x10 ⁷
2 - 7F	0.0723	3.18x10 ⁻³	0.3	2.1x10 ⁷
1F	0.1141	6.98x10 ⁻³	0.3	2.1x10 ⁷

1tonf=9.8kN

Table 2: Material Properties of Building (Beam)

Floor	A (m ²)	I (m ⁴)	ν	E (tonf/m ²)
14 - RF	0.0147	2.98x10 ⁻³	0.3	2.1x10 ⁷
9 - 13F	0.0169	3.46x10 ⁻³	0.3	2.1x10 ⁷
3 - 8F	0.0183	3.63x10 ⁻³	0.3	2.1x10 ⁷
2F	0.0182	6.84x10 ⁻³	0.3	2.1x10 ⁷
Foundation	2.8	3.73	0.16	7.3x10 ⁸

1tonf=9.8kN

Material properties of the cast-in-place concrete piles are shown in Table 3. The piles are treated as two node beam elements in the analysis. The diameter of piles is 2.2m and length is 30m.

Table 3: Material Properties of Pile

	A (m ²)	I (m ⁴)	ν	E (tonf/m ²)
Pile	3.8013	1.15	0.167	2.3x10 ⁸

1tonf=9.8kN

Table 4: Soil properties

Depth (m)	Gravity (Mg/m ³)	Porosity	G (tonf/m ²)	K (tonf/m ²)	Permeability m/sec
GL-0 - -3.5	2.65	0.588	4000.	1.20x10 ⁴	10 ⁻⁶
GL-3.5 - -20	2.65	0.588	4000.	1.20x10 ⁴	10 ⁻⁶
GL-20 - -30	2.65	0.588	7000.	1.61x10 ⁴	10 ⁻⁶
GL-30 - -40	2.65	0.442	50000.	6.95x10 ⁴	10 ⁻⁶

1tonf=9.8kN

Table 5: Soil properties

Case	Cohesion	ϕ	γ	A	B
NA015	0.0	30.0	6.0	0.15	600.
NA025	0.0	30.0	6.0	0.25	600.

Sandy soil is located from the surface to -20m depth and water table is at -3.5m. These layer below the water table is assumed to liquefy. The permeability is small so it might be considered undrain condition during earthquake excitation. The bottom 10m is more than ten times harder than the upper layers. The other layer except possible liquefying layer are considered elastic two phase material. Table 4 shows the elastic properties.

Elasto-plastic properties of soil is shown in Table 5. ϕ is the friction angle. γ , A and B are the parameters of the Densification model. These parameters are determined by a laboratory test.

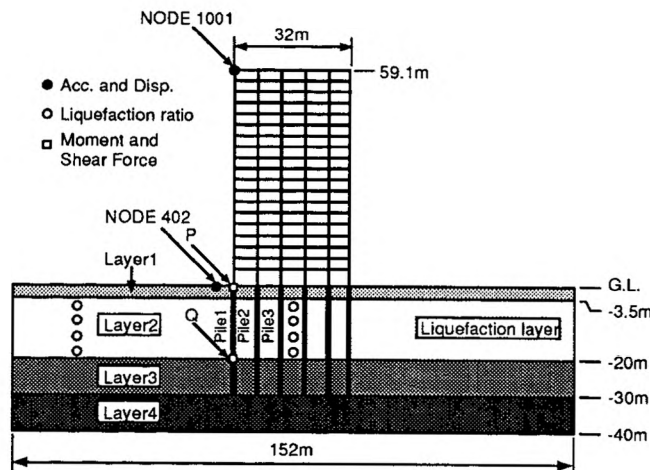


Figure 2: Overview of Pile-Soil-Structure Model

Soil constants for dilatancy are determined to fit a liquefaction strength curve (Strength vs N-value) by simulating a triaxial test. The simulation is conducted by a simple element test program with the same subroutines of the finite element code. It is difficult to obtain the exact curve fitted so two points, strength for 5 and 20 cycles, are used as a target value. Error is obtained comparing with the target points. The soil constants are not uniquely determined for a curve so we intuitively choose it examining the stress path behavior. The confining pressure 98kPa is used as a standard test procedure. The strength curves calculated are shown with the obtained soil parameters in Fig. 3. Strength is 0.1 for N=5 and 0.05 for N=20. The material can very easily liquefy since "0.3 for N=5 and 0.21 for N=20" are the liquefaction strength of ordinary sand which liquefies. In our survey, we assume the soil is very weak and can be liquefy with earthquake which surface acceleration is about 200 to 300 cm/sec².

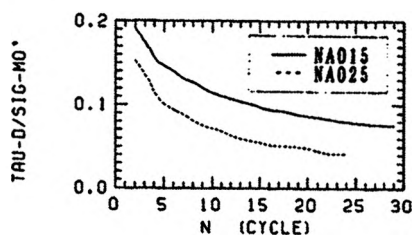


Figure 3: Liquefaction Strength Curve

Rayleigh damping matrix of for the form

$$C = \alpha M + \beta K \quad (6)$$

is used, in which M and K are the mass and the initial stiffness matrix, respectively. $\alpha = 0.1951$ and $\beta = 0.0089$ are used based on a 5 per cent damping ratio for the first two modes of eigenvalue analysis. Those constants α and β are not changed through the excitation of the earthquakes.

CHARACTERISTICS OF MODEL SYSTEM

Pile Behaviour by Static Lateral Force

Pile reaction in static condition is studied with the same finite element model which is used in the dynamic analyses. Fig. 4 shows

deformation pattern and bending moment of piles when unit lateral forces applied to each head of the piles.

Pile 1, 2 and 3 indices the pile number from the outside to inside. Both bending moment and deformation are almost same but the maximum bending moment at head of the pile 1 is slightly larger than the others. The reason of this is that pile 1 is less supported by the surrounding area than the pile 2 and 3. The deformation profile shows shear deformation pattern for pile 2 and 3. Moment deformation pattern for pile 1. Looking at the lower part of piles, slight discontinuity of the bending moment is seen at -20m because the layer -20m to -30m is harder than the upper layer. The maximum bending moment is appeared at the top of the piles and that of the rest piles is negligible.

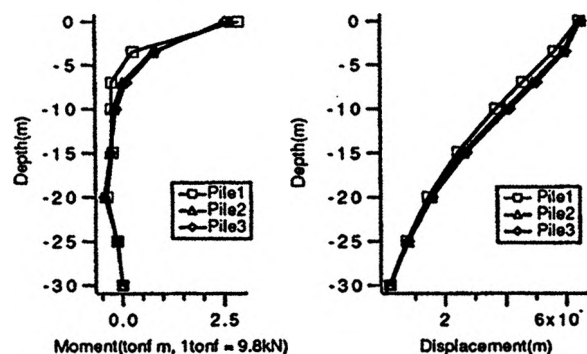


Figure 4: Bending Moment / Deformation in Static Case

Vibration Mode

Characteristics of the vibration is studied for the pile-soil-structure model using an eigenvalue analysis and a frequency response analysis. One phase problem is solved by the eigenvalue analysis since eigenvalue analysis for a two phase problem requires an unsymmetrical complex value eigenvalue solver. In this case, soil properties are considered as averaged material of fluid saturated porous material and solved assuming undrained condition. The natural frequencies obtained is shown in Table 6. The lowest frequency is 0.492Hz corresponding to building's first mode. The second lowest frequency is 1.30Hz which corresponds to the first mode of the soil layers. The natural frequencies for the two phase situation are obtained by the frequency domain analysis in order to know effects of interaction between solid and fluid phase. To perform this the following equation is directly solved assuming that the input force is sinusoidal gravitational wave ($e^{i\omega t}$).

$$\begin{bmatrix} M_s & 0 \\ 0 & M_f \end{bmatrix} \begin{bmatrix} \ddot{\mathbf{u}} \\ \ddot{\mathbf{U}} \end{bmatrix} + \begin{bmatrix} C_1 & -C_2 \\ -C_2^T & C_3 \end{bmatrix} \begin{bmatrix} \dot{\mathbf{u}} \\ \dot{\mathbf{U}} \end{bmatrix} + \begin{bmatrix} K + K_1 & K_2 \\ K_2^T & K_3 \end{bmatrix} \begin{bmatrix} \mathbf{u} \\ \mathbf{U} \end{bmatrix} = \begin{bmatrix} \mathbf{f}_u \\ \mathbf{f}_U \end{bmatrix} \quad (7)$$

The peak frequencies obtained by frequency domain analyses are also shown in Table 5. The values are slightly different from the eigenvalue analysis. The difference of the most of modes are about 2 per cent. Natural frequency for the building dominate mode is 0.492Hz against the peak frequency 0.50Hz and that 1.30Hz against 1.32Hz for ground. The 4th mode has about 4 per cent difference. The 4th mode is a coupling mode between piles and soil layers so that the frequency and phase difference is affected by damping. The first and second vibration mode are shown in Fig. 5. which is the real part of the frequency response. The first mode is identical to the modes obtained by the eigenvalue analysis. The second mode

is same mode but slightly different. The reason of this is that the second natural frequency is close to the third one and has some coupling. This can be seen in the phase diagram in Figs. 6 and 7. The transfer function of the building top (Fig. 6) is smooth. The phase changes 0 to -180, then -360 so on. But the transfer function of the ground surface shows different phase change. It changes 0 to -90 and then back to 0 and then -90. This may be caused by damping effects. Transfer function for frequency shows the sharp peak so that means the system has little damping.

The modes higher than 5th does not take major role. The amplitude of transfer functions are very small (Figs. 6 and 7). The transfer function of soil-pile coupling mode is also small in this model. Therefore pile and soil structure will mainly behave as one structure. When some layer is weakened by any reason such as liquefaction phenomena, pile-soil interaction may be large.

Table 6: Natural Frequencies

Mode	Peak Freq. (2 phase)	Natural Freq. (1 phase)	1 phase/ 2 phase	Mode type
1	0.5	0.492	1.02	Building 1st
2	1.32	1.30	1.02	Ground 1st
3	1.57	1.56	1.01	Building 2nd
4	2.3	2.21	1.04	Ground pile coupling
5	2.6	2.535	1.02	Ground Vertical

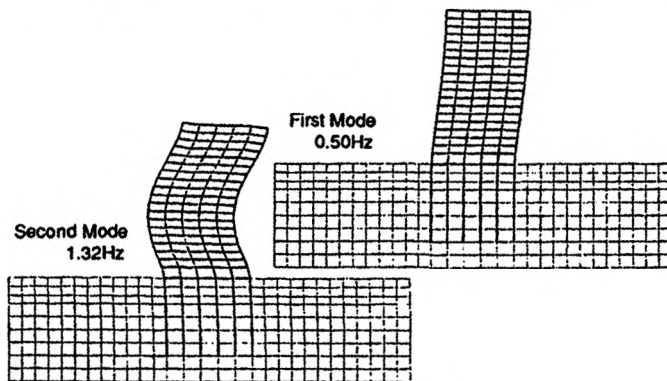


Figure 5: Vibration Modes

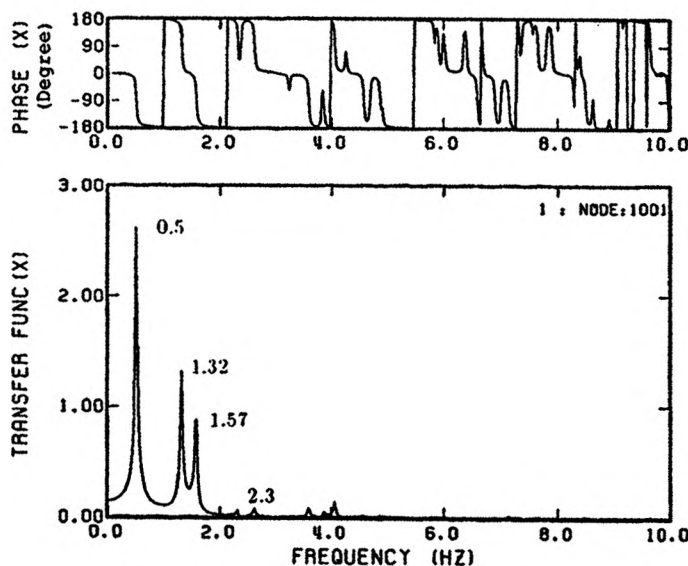


Figure 6: Transfer Function at Top of Building

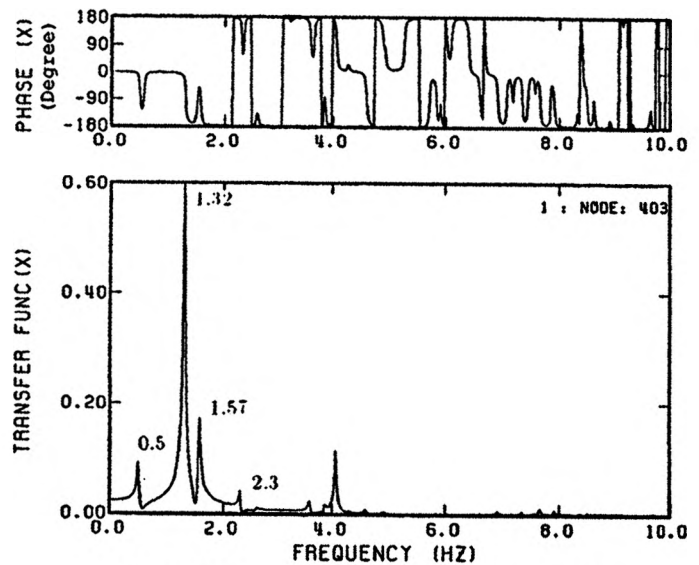


Figure 7: Transfer Function at Ground Surface

EARTHQUAKE RESPONSE ANALYSIS

Input motion

Three sets of recorded earthquake data are used for input motion of earthquake response analysis. An earthquake is a typical record of a strong earthquake. Rest two data were recorded at soft ground in Akita and Toyo (in Tokyo) but are not so large earthquake.

- (1) Niigata Earthquake 1964 NS recorded in Akita City(NS),
- (2) Chiba Earthquake 1989 recorded at Toyochi in Tokyo(EW),
- (3) Imperial Valley Earthquake 1940 at El Centro (NS).

Figs. 8 and 9 show the time history and Fourier Spectra of the earthquakes respectively. Earthquake Niigata and Chiba caused a lot of damage due to liquefaction phenomena and has similarity. Imperial Valley Earthquake is different type of earthquake which was recorded at a rock bad. The frequency spectra shows large amplitude from 1 Hz to 3 Hz. Among them, (1) shows rather small amplitude between 1.5 - 2.0 Hz. (2) shows small amplitude between 2.0 - 2.5 Hz. (3) shows almost the same amplitude upto 2.3 Hz.

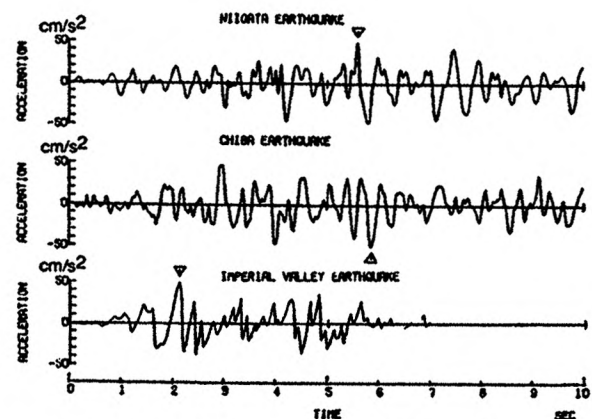


Figure 8: Time History of Input Motion

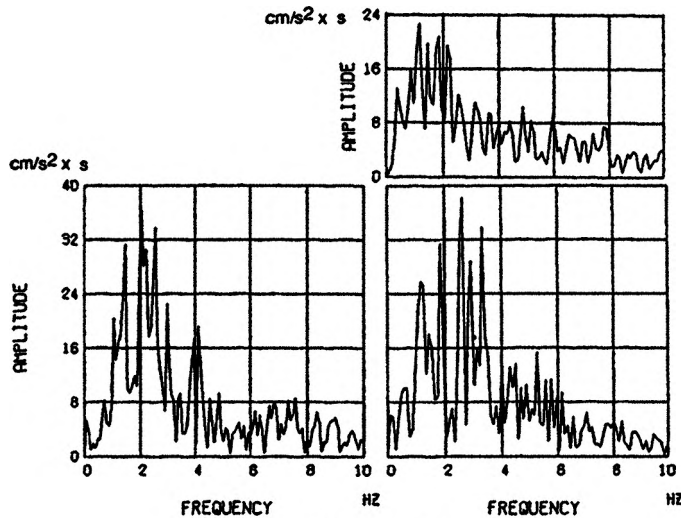


Figure 9: Frequency Spectra

The maximum acceleration of the input motion is set as 50 cm/sec² at the bottom of the model for all earthquakes. 10 seconds records are used for the analyses of earthquake (1) and (2). In the case of El Centro Earthquake, 7 seconds are used because the vibration ceases once around 7 seconds. As it is seen in the frequency analysis 1.31 Hz is dominant for ground peak. All earthquakes have strong amplitude around 1.3 Hz. El Centro could be the least one.

Liquefaction Ratio

Time history of liquefaction ratio are shown for points below and far from building in Fig. 10. The liquefaction ratio is defined by $1 - \sigma_m / \sigma'_{m0}$ where σ_m is mean effective stress at any time and σ'_{m0} is the initial effective mean stress. The liquefaction ratio is zero at the initial condition and is one when full liquefaction takes place. Figs. 10 and 11 show that full liquefaction takes place in free field and less liquefaction takes place in the points below the building. Full liquefaction takes place in all cases but the most earliest liquefaction is observed in case of Toyo earthquake. Speed of liquefaction is very much depend on the earthquake history.

Figs. 12 and 13 show the deformation profile for the three earthquake. The movement of surface ground around the building is largest in case of El Centro Earthquake. The movement is like a plate slides on fluid surface. The response movement for the Toyo Earthquake is entirely different from that for El Centro Earthquake. A compression/extension wave transfers for lateral direction along the surface. Its movement is large but it does little slide. Some typical deformation profiles are shown in Figs. 12 and 13.

It should be noticed that liquefaction can not be measured by only excess pore pressure built-up. But it should be measured by the reduction of effective stress such as liquefaction ratio because excess

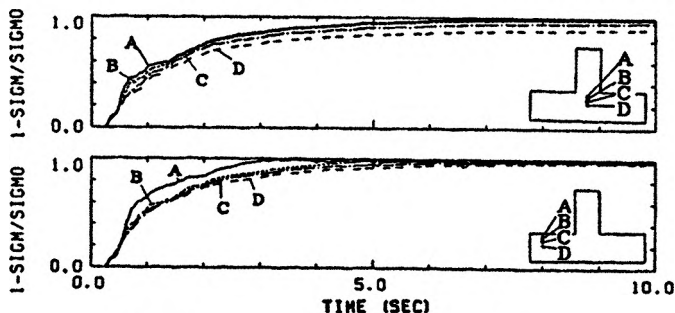


Figure 10: History of Liquefaction Ratio(Toyo)

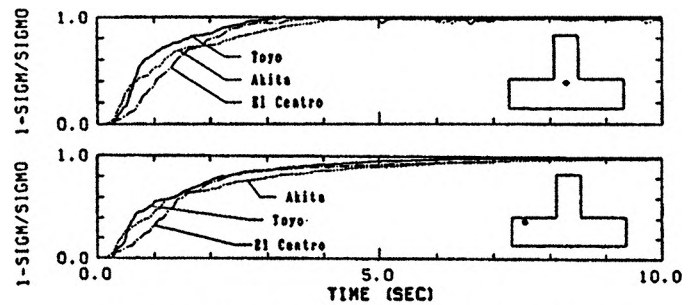


Figure 11: History of Liquefaction Ratio(2nd layer)

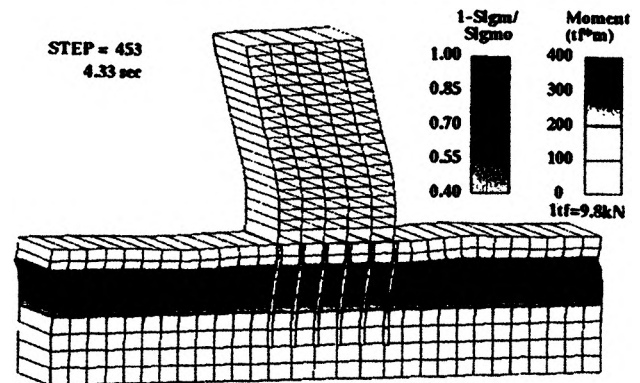


Figure 12: Deformation Profile for Toyo Earthquake

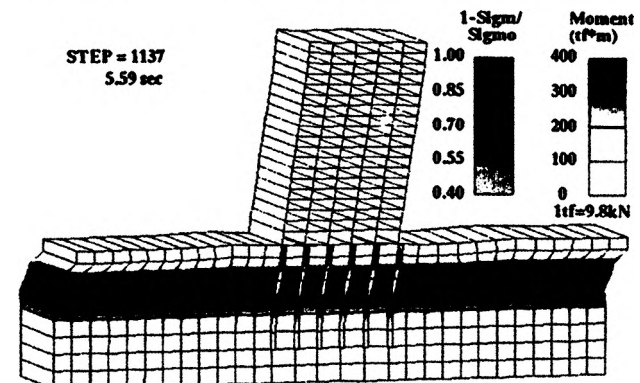


Figure 13: Deformation Profile for El Centro Earthquake

pore pressure is induced not only by liquefaction but also by compress movement due to the rotation of building and/or interaction between piles and soil.

Effects of Liquefaction

Four cases of analysis are studied to survey liquefaction effects, i.e. two liquefaction analyses and two linear analyses. (1)liquefaction analysis where complete liquefaction takes place, (2)liquefaction analysis where maximum liquefaction is about 0.9 per cent, (3)equivalent linear analysis with reduced stiffness for shallow layers, (4)linear analysis without any modification of material properties.

In the case 4, elastic modula are obtained by ordinary procedure of site investigation such as elastic wave test. Therefore material properties are only valid for very small strain. The stiffness reduction of the case 3 are one third of the case 4. The input motion is the Toyo Earthquake shown in Fig. 8. Fig. 14 shows a maximum response acceleration and displacement of the line of pile 3 and the side boundary of the soil layers for the above four cases. The two

liquefaction analyses show similar results but the complete liquefaction causes the less acceleration and displacement at the head of pile. Those may be caused the difference of degree of liquefaction. The liquefaction ratio of center soil is 89 per cent and of the side boundary 98 per cent. At the side boundary the complete liquefaction causes less response acceleration and larger displacement. But the differences are little so the tendency may be affected by variation of material properties and input motions. We survey for input motions later.

Linear analysis, case 4, give a entirely different profile of acceleration and displacement. The vibration is similar to the 3rd eigenmode while the other cases are similar to the 4th eigenmode.

The equivalent linear analysis, case 3, shows good correspondence to the liquefaction analysis but does not agree qualitatively. In this particular case, displacement response are almost same for the case 1 to 3.

Figs. 15 and 16 show a maximum response of bending moment and shear force of piles for Toyo earthquake. The analysis for Akita earthquake show similar results. Linear analysis, case 4, shows that the bending moment and shear force are entirely different profile in depth. They are larger than that of nonlinear analysis at the head of piles and smaller at the lower part of the piles. The case 1 to 3 shows similar results in the bending moment profile but the equivalent linear approach is different for the shear force.

When we look at the time history of acceleration and displacement difference of the analysis methods are obvious. Fig. 17 shows the time histories of acceleration and displacement at the top of the building and at the surface of ground near the building. Results of the three analyses are compared, i.e. linear, equivalent linear and liquefaction analyses. The wave shapes are different. The result of the liquefaction analysis has longer period of wave. This can not be simulated by equivalent linear analysis.

The Bending moments of the same analyses are compared. The magnitude of the three analyses are close as we see in Fig. 15 but wave behavior is entirely different as shown in Fig. 18 where the bending moment and shear force are shown for head (point P) and the point -20m (point Q) of pile 1. Particularly shear force is different from the linear results. This may be caused by loss of external force of the liquefied layer.

Linear analysis with stiffness reduction shows better agreement to the liquefaction analysis as a whole. The bending moment, shear force, acceleration and displacement at top part of piles behave similarly to liquefaction analysis. But behavior of those at the lower part is different from the nonlinear analysis. One of the reason for this may be that the reduction of stiffness is not properly assumed

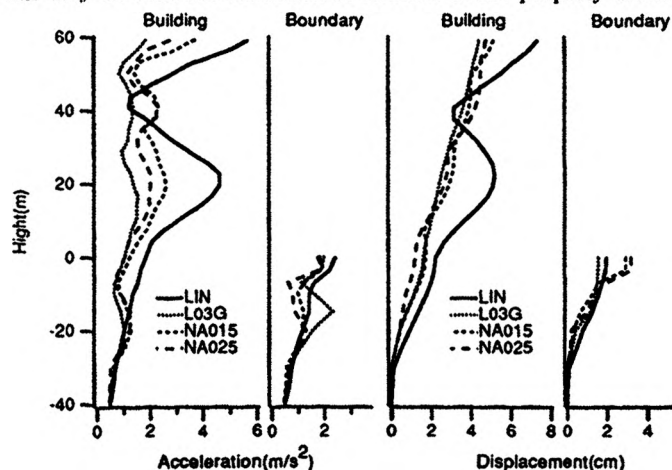


Figure 14: Max. Acc. and Disp for Toyo Earthquake

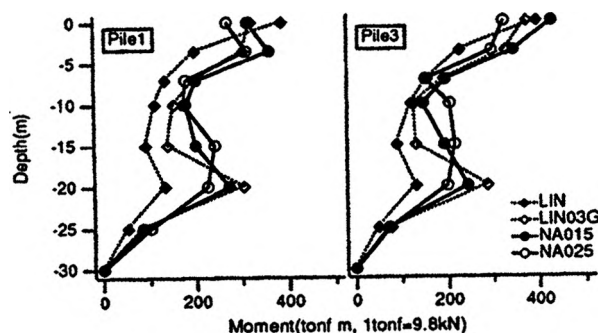


Figure 15: Bending Moment of Piles

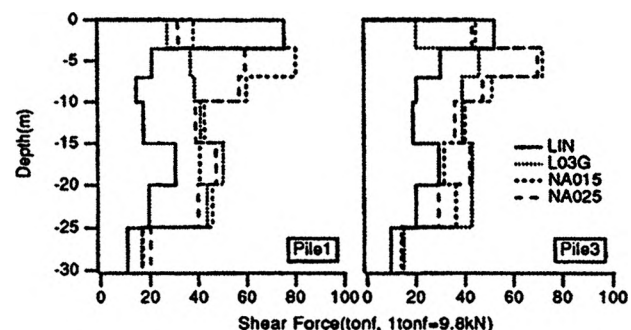


Figure 16: Shear Force of Piles

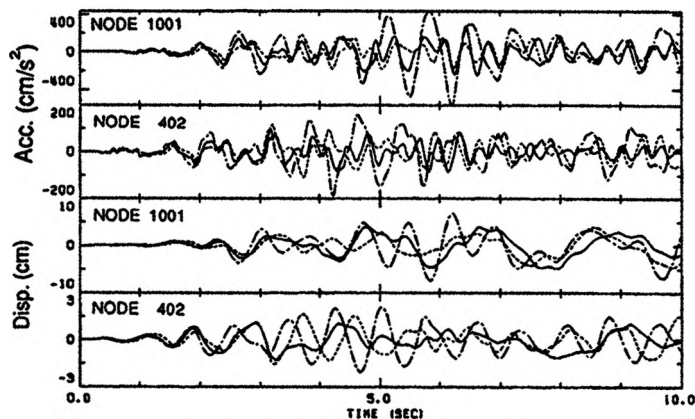


Figure 17: History of Acc./Displacement

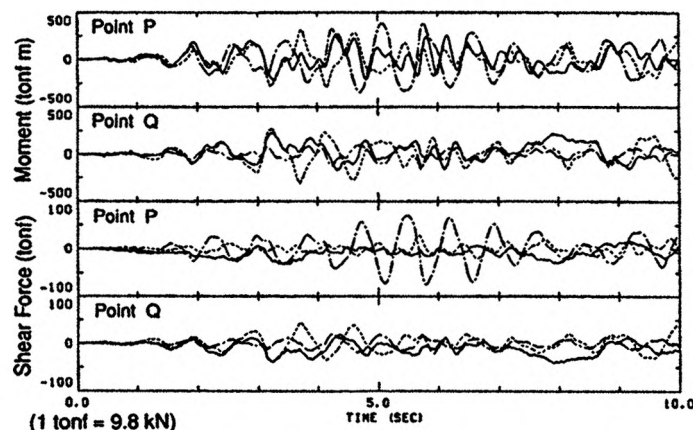


Figure 18 : History of Bending Moment / Shear Force

and the same reduction ratio is used for any location of the layer. Liquefaction ratio at the bottom of the building is less than the free field layer. Therefore linear analysis with stiffness reduction of possible liquefaction layer is not appropriate to design purpose in any case.

Equivalent Linear Analysis

The words "equivalent linear analysis" is often used in frequency domain analysis. Equivalent shear modulus and damping ratio is calculated as a function of the maximum strain which is obtained by previous calculation. And the calculation is repeated using the new shear modulus and damping ratio until it converge.

The same idea can be used in time domain analysis if the calculation is repeated several times. Although the time domain analysis is expensive in a computational aspect it is possible to iterate several times. The densification model can be used for the purpose, i.e. calculating the stiffness reduction ratio according to the autogeneous strain of the previous calculation.

We examine the equivalent linear method simulating the liquefaction phenomena for the three input motions mentioned in Fig. 8. In this example the shear modulus is reduced to one third of the original value. Since no formula has not been found yet to determine the reduction ratio of the shear modulus depending upon accumulated shear strain for this equivalent linear analysis, we take this intuitively. When liquefaction is take place, the shear modulus become zero. But zero modulus will not produce correct results because it has resistance until the full liquefaction takes place which is well-after 2 or 3 second. But the ratio should be examined in more details.

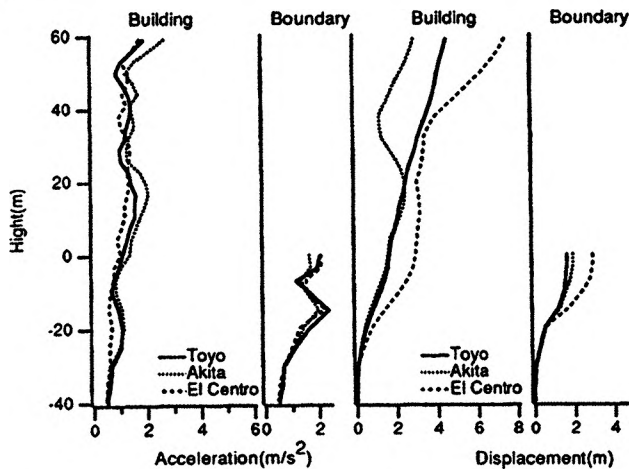


Figure 19: Max. Acc./Disp. Equivalent Linear Approach

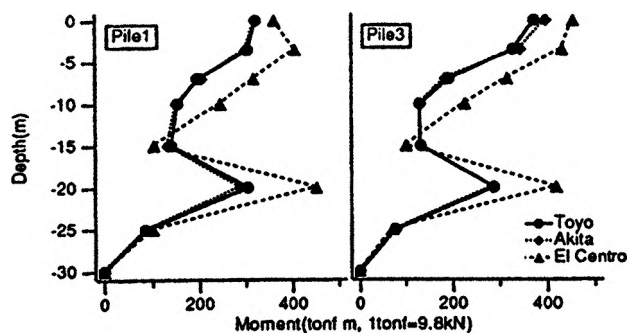


Figure 20: Bending Moment of Equivalent Linear Approach

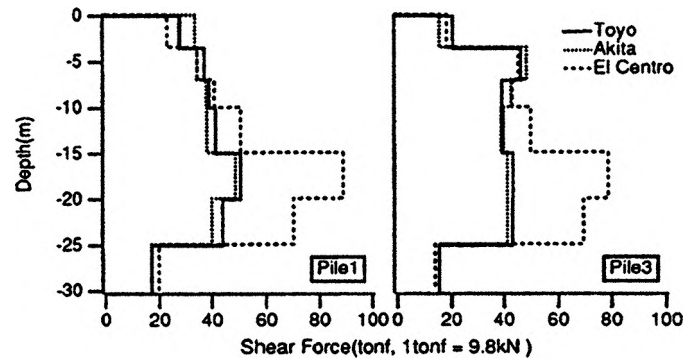


Figure 21: Shear Force of Equivalent Linear Approach

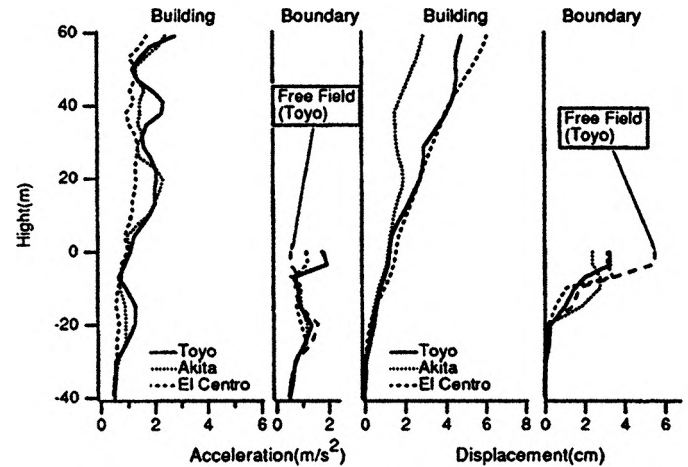


Figure 22: Max. Acc./Disp. Equivalent Linear Approach

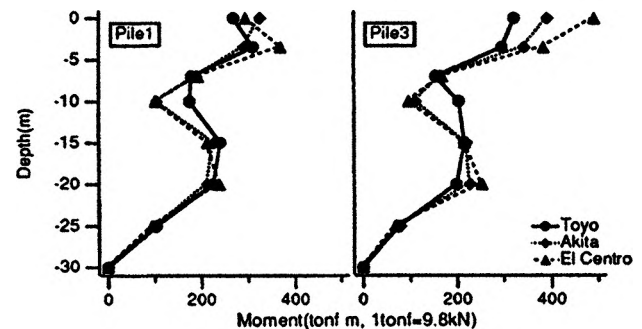


Figure 23: Bending Moment of Piles

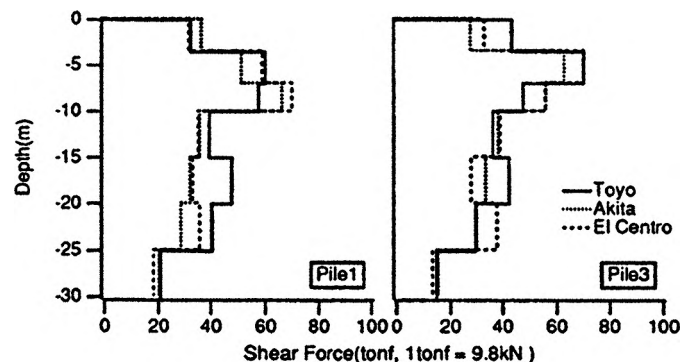


Figure 24: Shear Force of Piles

Results with the reduced shear modulus are shown for the maximum values of acceleration and displacement in Fig. 19, the bending moment in Fig. 20 and shear force in Fig. 21. The same set of results for the liquefaction analysis (NA025) are shown in the following figures (Figs. 22, 23 and 24). Comparing the both results, it might conclude that the equivalent linear approach shows qualitatively good agreement. For example the maximum acceleration and displacement of the building and the piles show the same profile with the results of NA025 but the Shear force profile along the piles shows the different tendency. In the case of Akita Earthquake, the maximum response accelerations along the building and piles are very close but are different in the free field.

In our example, the piles and the building are linear therefore it obtain rather good results but the soil layers are non-linear material and does not obtain good agreements of the both analyses.

The equivalent linear analysis can be used only when nonlinearity is not too high. And it can be used only if engineers knows how to interpret the data, results and the limitation. The accurate evaluation of the stiffness reduction is critical. To do this correctly, a dynamic analysis is required to calculate build-up pore pressure simultaneously but it does not make sense for equivalent method. If a simple approach is found to estimate proper liquefaction ratio and a reduction rule of the stiffness, the method has full advantage to solve liquefaction problems.

Influence of Liquefaction to Piles

The existence of liquefied layer makes the vibration behavior complex as mentioned above. In the case of Toyo Earthquake vibration mode for liquefaction become one mode higher. The acceleration profile of soil layers shows the 3rd mode from the 1st mode (no damage linear). The 3rd mode for the building is up to the 5th mode. As the result of this tendency, the maximum deformation of the building is reduced. This higher mode is seen in the results of the equivalent linear analysis so existence of sandwiched thin and very soft layers causes vibration mode higher. And low frequency component of the input motion is filtered through the soil layers. It will make the building safer but will make the pile critical as Fig. 15 shows. These tendency is confirmed for other earthquake. Three sets of earthquake are surveyed. Acceleration and displacement of free field are shown in Fig. 22. All response are in high frequency modes. The building vibrate in the 6th mode in case of Toyo Earthquake and the 4th mode in case of Akita and El Centro Earthquake. The vibration mode of the free field is slightly different from the coupled problem. The vibration mode of soil layer is the 3rd mode without liquefaction since the elastic modula are depth dependent. Therefore the mode is not changed but the shape is made sharp and clear.

In this analyses the side boundary is tied between right to left side so it can not represent infinity. The difference due to this assumption is seen on maximum acceleration and displacement profile (Fig. 22).

Fig. 23 shows the bending moment of pile 1 and pile 3. The bending moments at the head of pile 3 are vary for the input motions but not the lower parts of the piles.

The liquefied layers do not transfer shear wave. So resistance of soil against pile become very small. But the surface layer behave as normal elastic material. Therefore the force to the piles acts only at the surface layer. Fig. 24 shows that tendency i.e. shear force of the pile is almost constant from -10m to -20m. This tendency is not seen in the case of equivalent linear analysis (Fig. 21).

Different earthquake cause some difference in all the aspects of response. The differences are as much as the ordinary elastic response analysis. But the results of liquefaction analysis is entirely different from the results of linear analysis. So liquefaction analysis is essential.

CONCLUSIONS

The following conclusions are derived by investigating a particular example of a pile-soil-structure system subjected to the liquefaction phenomena due to three kinds of earthquake.

Nonlinear liquefaction analysis must be used if full liquefaction is anticipated. It will affect both building and foundation design.

Liquefaction causes considerable reduction of shear resistance and produce a thin and very soft layer. This layer acts a kind of low frequency cut filter and induces higher frequency mode of the building movement. This may take the current design safer side for the building but critical side for the piles design.

Equivalent linear analysis is surveyed in comparison with liquefaction analysis. The methods show qualitative agreement and an iterative time domain approach is suggested to obtain better agreement. In any case, however, analysts should understand the limitation and the characteristics of the method.

Frequency analysis for two phase material is presented. It provides important preparatory information for analysts.

This report concentrates on the situation in case of full liquefaction. The case of partial liquefaction and prediction of liquefaction will be discussed separately.

REFERENCES

- Tokitou, K. et. al. (1989), 'Cell Type foundation Improved by Deep Cement Mixing Method against Soil Liquefaction, Part5: A Case Study of Design: 19 Story Building Foundation Supported by Piles', *Proc. of Congress of Architectural Institute of Japan*.
- Bazant, Z.P. and Krizek, R.J., (1976), 'Endochronic constitutive law for liquefaction of sand', *Proc. Amer. Soc. Civ. Eng. J. of Eng. Mech. Div.* 102(EM4), 701-22.
- Finn, W.D.L., Lee, K.W. and Martin, G.R. (1977), 'An Effective Stress Model for Liquefaction', *J. of Geotechnical Engineering Division, ASCE*, Vol. 103, No. GT6, pp.517-533.
- Ishihara, K. and Towhata, I., (1980), 'One-Dimensional Soil Response Analysis during Earthquakes Based on Effective Stress Analysis', *J. of the Faculty of Engineering, University of Tokyo*, Vol. 35, No. 4, pp.655-700
- Muto, M., et. al. (1990), 'Applicability of Liquefaction Analysis (No.3: Shaking Table Test and Analysis of Soil System)', *The 25th Japan National Conf. on Soil Mech. and Foundation Engineering, Okayama, Japan*, pp.995-998
- Penzien, J., (1970), 'Soil-Pile Foundation Interaction', *Earthquake Engineering*, Ed. by R.L. Wiegell, Englewood Cliffs, N.J.: Printice-Hall
- Shiomi, T., Hirose, T. and Tanaka, Y., (1988), 'A Study of An Approximate Formulation for Fluid Saturated Porous Media', *Proc. of Symposium in Computational Mechanics*, Ed. Nikka Giren, Tokyo.
- Tanaka, T. and Yasunaka, M. (1982), 'Dynamic Response Analyses and Shaking Table Tests', *Proc. of the 4th Int. Conf. Num. Method in Geomech.*, Ed. Eisenstain, Z., Edomonton, Canada, pp. 459-468.
- Zienkiewicz, O.C., Chang, C.T. and Hinton, E. (1978), - 'Nonlinear seismic response and liquefaction', *Int. J. Num. and Anal. Meth. in Geomech.*, Vol.2, No.4, pp.381-404.
- Zienkiewicz, O.C. and Shiomi, T. (1984), 'Dynamic Behaviour of 'Saturated Porous Media; The Generalized BIOT formula and its Numerical Solution', *Int. J. for Numerical and Analytical Methods in Geomechanics*, Vol.8, 71-99.